JOURNAL OF AIRCRAFT
Vol. 44, No. 3, May–June 2007

Engineering Notes

ENGINEERING NOTES are short manuscripts describing new developments or important results of a preliminary nature. These Notes should not exceed 2500 words (where a figure or table counts as 200 words). Following informal review by the Editors, they may be published within a few months of the date of receipt. Style requirements are the same as for regular contributions (see inside back cover).

Dynamic Coupling of the KC-135 Tanker and Boom for Modeling and Simulation

Austin L. Smith*
U.S. Air Force Research Laboratory, Wright-Patterson Air Force Base, Ohio, 45433
and
Donald L. Kunz†
U.S. Air Force Institute of Technology, Wright-Patterson Air Force Base, Ohio, 45433

DOI: 10.2514/1.27241

Nomenclature

A	=	direction cosine transformation matrix
B	=	velocity transformation matrix
C_D	=	ruddevator cross-sectional drag coefficient
C_L	=	ruddevator cross-sectional lift coefficient
c	=	ruddevator cross-sectional chord
D	=	Jacobian of the vector of constraint equations
F	=	aerodynamic force vector, floating joint velocity transformation block matrix
I	=	inertia/mass matrix
M	=	aerodynamic moment vector
m	=	mass
n	=	unit vector
P	=	prismatic joint velocity transformation block matrix
p	=	generalized velocity vector
Q	=	generalized force/moment vector
q	=	generalized displacement vector
r	=	position vector
U	=	universal joint velocity transformation block matrix
u_E	=	displacement of the boom extension (positive extending)
V_x	=	ruddevator cross-sectional velocity in the x direction
V_y	=	ruddevator cross-sectional velocity in the y direction
V_z	=	ruddevator cross-sectional velocity in the z direction
v	=	velocity vector
α	=	ruddevator cross-sectional angle of attack
Δ	=	identity matrix
η	=	vector of joint coordinates
θ	=	ruddevator pitch angle
λ	=	vector of Lagrange multipliers
ρ	=	air density
Φ	=	vector of constraint equations
ϕ	=	ruddevator cross-sectional flow angle
ψ	=	ruddevator cross-sectional yawed flow correction
ω	=	angular velocity vector
$\dot{()}$	=	derivative with respect to time
$\tilde{()}$	=	skew-symmetric matrix defined such that $\tilde{a}^T = -\tilde{a}$

Subscripts

B	=	tanker
E	=	boom extension
F	=	fixed boom
R	=	ruddevator
S	=	system
θ	=	fixed boom pitch
ψ	=	fixed boom yaw

Superscripts

B	=	tanker
E	=	extension
I	=	inertial space
X	=	placeholder

I. Introduction

FUTURE unmanned aerial vehicle (UAV) missions will include overseas and long-range flights that require aerial refueling. Refueling UAVs en route introduces new tactical, operational, and safety issues not encountered in manned aircraft aerial refueling operations [1]. To address these issues and to train personnel involved in the refueling process, advanced high-fidelity models and simulations are necessary. High-fidelity analytical models of the KC-135 tanker, shown in Fig. 1, the refueling boom, and the UAVs currently exist separately, but no existing single system models the dynamic interactions between them.

To improve the modeling of automated aerial refueling and accurately simulate the refueling process, the dynamic interactions of the three bodies must be integrated. This Note will specifically address the tanker–boom interactions and how to model them for simulation purposes. A new integrated analytical model will be developed that incorporates aircraft motion effects into the boom equations of motion and aerodynamics, and the boom forces and moments will, in turn, be transmitted to the tanker.

The KC-135 aerial refueling boom is attached to the aircraft at the boom root by a vertical pin and a yoke-and-trunnion assembly, a combination known as the boom fork, shown in Fig. 2 [2]. The pin, assumed to be aligned with the vertical aircraft axis, allows yawing movement, and the yoke-and-trunnion assembly, attached to the pin, allows pitching movement. The fixed portion of the boom is attached to the boom fork and extends 27 ft, 8 in., and ends in an enlarged fairing to which two control surfaces, called ruddevators, are attached. The ruddevators each have a 31-in. chord and a 61-in. span and are mounted at a 42-deg dihedral angle. They allow the boom operator to fly the boom to the receiver aircraft's receptacle and also help to alleviate loads on the boom and bending during connected flight. A mechanical pantograph system [3] consisting of cables and

Presented as Paper 6480 at the AIAA Modeling and Simulation Technologies Conference and Exhibit, Keystone, CO, 21–24 August 2006; received 11 August 2006; revision received 9 January 2007; accepted for publication 23 January 2007.

*Associate Aerospace Engineer, Air Vehicles Directorate, 2180 Eighth Street. Member AIAA.
†Associate Professor, Department of Aeronautics and Astronautics, 2950 Hobson Way. Associate Fellow AIAA.

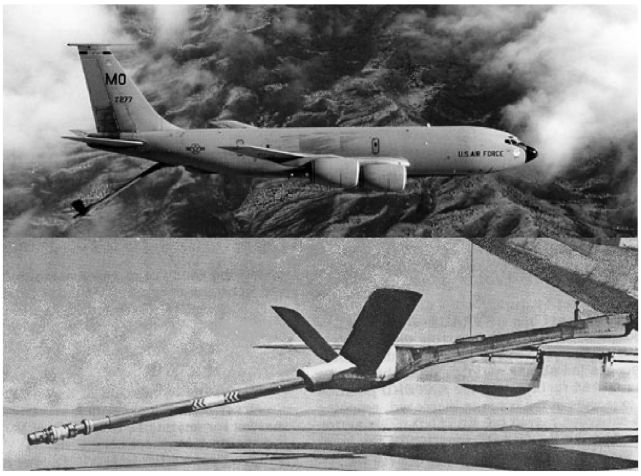

Fig. 1 KC-135 tanker and refueling boom.

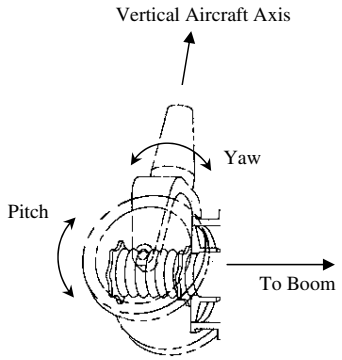

Fig. 2 Boom fork.

pulleys positions the ruddevators nearly parallel to the airstream, a process known as autorotation, keeping them at low angles of attack and alleviating air loads on the boom without input from the boom operator. This is accomplished by rotating them as a function of boom yaw and pitch. An extendable portion of the boom, 27-ft long, retracts completely inside the fixed boom and extends up to 20 ft outside the fixed boom. The boom extension ends in a nozzle for fuel transfer. The boom operator further deflects the ruddevators and extends or retracts the boom using two control levers in the boom operator station, a compartment forward of the boom fork on the underside of the KC-135.

II. Existing Models

The current analytical models used for simulating automated aerial refueling at the U.S. Air Force Research Laboratory (AFRL) consist of a high-fidelity Boeing KC-135 model and the boom operator part task trainer (BOPTT) boom model, a model developed for the Air Education and Training Command and used in a boom operator training simulator. The boom model is attached geometrically to the tanker at the boom root and behaves as though the attachment point is translating through the air on an imaginary rigid rail. The BOPTT equations of motion (EOM) and aerodynamic buildup as they are implemented into the AFRL simulation do not allow for dynamic interactions with the tanker aircraft. BOPTT aerodynamic and gravitational terms are directly applied to moment equations and do not straightforwardly provide forces that are necessary for a coupled model. Furthermore, the tanker model is not affected by any boom dynamics. Although limited in its capacity to advance aerial refueling research beyond the current state, the BOPTT model was built on experimental data and its behavior has been evaluated by boom operators at the AFRL. Accordingly, the uncoupled dynamic responses of the BOPTT are used to validate the new boom model's dynamics.

Another existing boom model was developed at the U.S. Air Force Institute of Technology (AFIT) and used for research on how to increase the operational capability of the boom with today's new receiver aircraft. This model, based on empirical aerodynamics, also does not take into account coupling effects with the tanker, but does include pertinent physical characteristics and information needed for the new model's development, such as boom and ruddevator dimensions, boom component weights, and ruddevator airfoil information. The dynamic simulation using this model focused on ideal refueling conditions and assumed a fixed boom extension for each simulation run. Consequently, for comparisons with the BOPTT and the new model, this model was modified to include boom extension and retraction during a simulation.

III. Coupled Tanker/Refueling Boom Analytical Model

There are a number of methods that can be used to derive the equations of motion for an analytical model of the tanker/refueling boom system. The rationale for choosing the method described next was driven by the desire to ensure as much compatibility as possible between the new boom model and an existing model of the KC-135 tanker to which the new boom model will be coupled.

The equations of motion for the existing KC-135 tanker model are written in the form shown in Eq. (1), in which the tanker is modeled as a rigid body, and the aerodynamic force and moment vectors on the right-hand side of Eq. (1) are functions of the aircraft states (velocities and displacements) and the pilot control inputs. The tilde operator in Eq. (1) and subsequent equations represents a skew-symmetric matrix formed from the underlying vector [4]:

$$\begin{bmatrix} m_B\Delta & 0 \\ 0 & I_B \end{bmatrix} \begin{Bmatrix} \dot{v}_B \\ \dot{\omega}_B \end{Bmatrix} = \begin{Bmatrix} F_B \\ M_B - \tilde{\omega}_B I_B \omega_B \end{Bmatrix} \tag{1}$$

Equation (1) is solved, as in the tanker model, by first calculating the aircraft accelerations by multiplying both sides by the inverse of the aircraft inertia matrix. Then, the accelerations are integrated to get the velocities that are, in turn, integrated to get the aircraft displacements. Before the second integration, the angular velocities must be transformed to aircraft attitude rates. Given this formulation and solution of the equations of motion for the tanker alone, a compatible form of the equations of motion for the coupled tanker/boom system is desired.

Therefore, in the present model, the equations of motion for the tanker are written exactly as shown in Eq. (1). The origin of the tanker coordinate system is located at the mass center of the aircraft, and the axes correspond to the standard aircraft coordinate system (x positive forward, y positive to starboard, and z positive down; see Fig. 3).

The method chosen for formulating and solving the equations of motion for the refueling boom and coupling them to the tanker equations employs an implementation of joint coordinates and the velocity transformation [5,6]. Joint coordinates are the coordinates that correspond to the motion permitted by each joint. The velocity transformations are expressions that transform the time derivatives of the joint coordinates into the absolute velocities and angular velocities, with respect to the inertial reference frame, of each body in the system. This method permits the independent derivation of the equations of motion for each body in the system. Those equations are

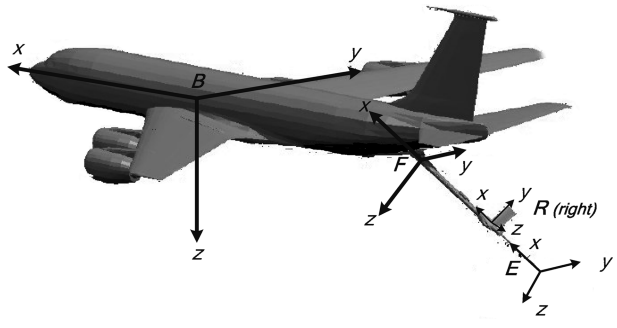

Fig. 3 KC-135 and refueling boom coordinate systems.

subsequently coupled to one another to form a system of equations in a form analogous to that shown in Eq. (1).

A. Refueling Boom

The refueling boom is modeled as two rigid bodies: a fixed boom and a boom extension, which are connected to one another. The fixed boom is fixed only in the sense that one end is attached to the tanker fuselage at the boom pivot, about which the fixed boom is permitted to yaw and pitch relative to the fuselage. Control of the fixed boom is facilitated by two ruddevators that are attached to the fixed boom near its free end. The ruddevators are also modeled as rigid bodies, each of which is controlled in pitch about its axis of aerodynamic centers. The boom extension telescopes out of the fixed boom along an axis parallel to the longitudinal axes of the fixed boom and boom extension.

1. *Fixed Boom*

The origin of the fixed boom coordinate system is located at the boom pivot, not at its mass center. The axes of the fixed boom coordinate system are defined such that when the boom yaw and pitch angles are zero, the boom axes are aligned with the tanker axes. Therefore, the x axis points in the direction of the boom pivot when viewed from the boom tip, the boom pitches about the y axis, and the z axis nominally points down at zero pitch.

Mass and inertia properties for the fixed boom were derived from, but are not identical to, the mass and inertia properties described in [2], because the author models the entire refueling boom as a single body with variable mass and inertia properties. Using the weight breakdown contained in [2], the weights of the fixed boom components are listed in Table 1. Moments of inertia for the fixed boom are calculated assuming that fixed masses are point masses and that distributed masses are slender rods. Equation (2) contains the equations of motion for the fixed boom. Note that the form of Eq. (2) differs slightly from Eq. (1) in that the mass/inertia matrix in Eq. (2) includes off-diagonal block matrices and the force on the right-hand side includes an additional mass term. These additional terms appear because the origin of the fixed boom coordinate system is not located at the mass center of the fixed boom. The location of the mass center is indicated by an asterisk in the coordinate system subscripts in Eq. (2).

$$\begin{bmatrix} m_F\Delta & -m_F\tilde{r}_{F^*/F} \\ m_F\tilde{r}_{F^*/F} & I_F \end{bmatrix} \begin{Bmatrix} \dot{v}_F \\ \dot{\omega}_F \end{Bmatrix} = \begin{Bmatrix} F_F - m_F\tilde{\omega}_F\tilde{\omega}_F r_{F^*/F} \\ M_F - \tilde{\omega}_F I_F \omega_F \end{Bmatrix} \quad (2)$$

On the right-hand side of Eq. (2) are force and moment terms due to gravity, aerodynamic drag, and aerodynamic forces on the ruddevators. Calculation of the forces and moments due to gravity are straightforward. The calculation of the aerodynamic drag on the fixed boom is not difficult, but a couple of issues must be addressed.

Table 1 Fixed boom weight breakdown

Items	Weight, lbm	C.G. (in from pivot)
Snubber		
Hydraulic motor drive		
Stowage provisions		
Instrumentation		
Attaching provisions	122.5	0.0
Structure tube		
Fairing		
Hydraulics		
Fixed inner tube		
Electrical	427.3	
Fuel system	(distributed)	166.0
Ruddevators and supports		
Recoil assembly		
Ruddevator controls		
Ruddevator locking		
Dumping provisions	329.2	310.5

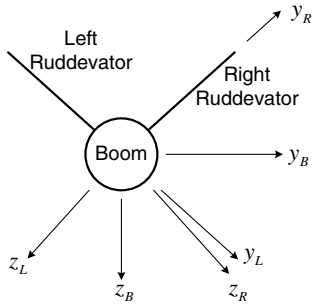

Fig. 4 Ruddevator coordinate systems.

First, the fixed boom fairing is not cylindrical, but rather is elliptical, to reduce the drag in the freestream direction. In addition, the fairing bulges significantly near the location of the ruddevators. To more accurately calculate the aerodynamic loads on the fixed boom, one should account for the fact that the cross section is elliptical and that the flow direction is not necessarily parallel to the major axis of the ellipse, and one should also account for the enlarged fairing cross section. For this investigation, only the average diameter of the fixed boom was available at certain lengthwise locations, making it impossible to model the elliptical boom cross section and enlarged fairing. Therefore, the aerodynamic loads on the fixed boom are calculated as one would calculate the drag on a circular cylinder. Only forces due to the velocity normal to the boom x axis are considered to produce drag forces. An implication of assuming a circular cross section with the average diameter is an underprediction of drag when the boom is yawed, increasing its predicted effective envelope, and an overprediction of drag in the streamwise direction.

Forces and moments on the ruddevators are calculated from aerodynamic strip theory. The origin of the coordinate system associated with each ruddevator is on the fixed boom centerline, on the point at which the pitch axis intersects it. Thus, the x axis for each ruddevator is oriented in the same direction as the fixed boom x axis, the y axis is collinear with the ruddevator pitch axis, and the z axis is nominally down before the dihedral rotation. To account for the 42 deg of dihedral for the ruddevators, the coordinate system for the left ruddevator is rotated 42 deg about the x axis, and the coordinate system for the right ruddevator is rotated -42 deg. As a result of the rotation of the coordinate system for the left ruddevator, the positive direction of the y axis is inboard from the tip, whereas for the right ruddevator, the positive direction of the y axis is outboard toward the tip. The ruddevator coordinate systems can be seen in Fig. 4.

Lift and drag forces are calculated at ruddevator cross sections, then integrated over the span of each ruddevator to obtain the forces and moments at the origin of the ruddevator coordinate systems.

$$F_R = \begin{Bmatrix} -\frac{1}{2}\rho c \int \left(V_x^2 + V_y^2 + V_z^2\right) C_D \, \mathrm{d}y \\ 0 \\ -\frac{1}{2}\rho c \int \left(V_x^2 + V_y^2 + V_z^2\right) C_L \, \mathrm{d}y \end{Bmatrix} \quad (3)$$

$$M_R = \begin{Bmatrix} -\frac{1}{2}\rho c \int \left(V_x^2 + V_y^2 + V_z^2\right) C_L y \, \mathrm{d}y \\ 0 \\ \frac{1}{2}\rho c \int \left(V_x^2 + V_y^2 + V_z^2\right) C_D y \, \mathrm{d}y \end{Bmatrix} \quad (4)$$

The lift and drag coefficients of the ruddevators' NACA 65_1-012 airfoil used in Eqs. (3) and (4) are interpolated from airfoil tables in which the coefficients are tabulated as functions of both angle of attack and Mach number. The angle of attack calculated at each cross section includes a correction for yawed flow, which is implemented as shown in Eqs. (5–7).

$$\psi = \frac{|V_x|}{\sqrt{V_x^2 + V_y^2}} \quad (5)$$

Table 2 Boom extension weight breakdown

Items	Weight, lbm	C.G. (in from pivot)
Rollers and supports	23.4	u_E
Inner tube		
Tube lining	375.1	
Fuel	(distributed)	$u_E + 165.0$
Nozzle		
Shock absorber	62.0	$u_E + 330.0$

$$\phi = \tan^{-1}\left[\frac{V_z}{\text{sgn}(V_x)\sqrt{V_x^2 + V_y^2}}\right] \tag{6}$$

$$\alpha = \tan^{-1}\left(\frac{\psi \sin\theta}{\cos\theta}\right) - \phi \tag{7}$$

Finally, the forces and moments for each ruddevator are transformed to act at and about the boom pivot and are combined with the forces and moments due to gravity and aerodynamic drag. In this manner, a vector of forces and a vector of moments are constructed for use in Eq. (2).

2. Boom Extension

The origin of the boom extension coordinate system is located at the inboard end of the boom extension. The axes of the boom extension coordinate system are defined such that they are always aligned with the fixed boom axes. Therefore, the boom extension telescopes in the direction of the x axis.

Mass and inertia properties for the boom extension were also derived from the weight breakdown contained in [2] and are listed in Table 2. In addition to the items listed in Table 2, the fixed boom fills with fuel at the rate of 0.39 lbm/in. as the boom is extended, replacing the volume vacated by the boom extension. Instead of bookkeeping the weight of this additional fuel with the fixed boom, it is included in the boom extension breakdown so that the properties of one body (fixed boom) are not dependent on the state of another body (boom extension). Therefore, the mass m_E, mass center r_E, and moments of inertia I_E of the boom extension are functions of its position relative to the boom pivot. Like the fixed boom, moments of inertia for the boom extension are calculated assuming that fixed masses are point masses and that distributed masses are slender rods. The resulting equations of motion for the boom extension are shown in Eq. (8). Equation (8) also includes the off-diagonal block matrices in the mass/inertia matrix and the additional mass term on the right-hand side, which result from the origin of the coordinate system not being located at the mass center.

$$\begin{bmatrix} m_E\Delta & -m_E\tilde{r}_{E^*/E} \\ m_E\tilde{r}_{E^*/E} & I_E \end{bmatrix}\begin{Bmatrix} \dot{v}_E \\ \dot{\omega}_E \end{Bmatrix} = \begin{Bmatrix} F_E - m_E\tilde{\omega}_E\tilde{\omega}_E r_{E^*/E} \\ M_E - \tilde{\omega}_E I_E \omega_E \end{Bmatrix} \tag{8}$$

The force and moment terms on the right-hand side of Eq. (8) are due to gravity and aerodynamic drag. Calculation of the forces and moments due to gravity are straightforward, once the mass and center of mass for the boom extension are determined, based on its position. The aerodynamic drag calculation is slightly more complex than the drag calculation for the fixed boom, because the only portion of the boom extension that is subject to drag is that portion that extends beyond the fixed boom. The extension beyond the fixed boom is treated as a circular cylinder and, like the fixed boom, only the velocity normal to the x axis is considered to produce drag.

B. Coupled Tanker/Refueling Boom Equations of Motion

The uncoupled equations of motion for the tanker, fixed boom, and boom extension are combined into a single set of equations, as shown in Eq. (9).

$$\begin{bmatrix} m_B\Delta & 0 & 0 & 0 & 0 & 0 \\ 0 & I_B & 0 & 0 & 0 & 0 \\ 0 & 0 & m_F\Delta & -m_F\tilde{r}_F & 0 & 0 \\ 0 & 0 & m_F\tilde{r}_F & I_F & 0 & 0 \\ 0 & 0 & 0 & 0 & m_E\Delta & -m_E\tilde{r}_E \\ 0 & 0 & 0 & 0 & m_E\tilde{r}_E & I_E \end{bmatrix}\begin{Bmatrix} \dot{v}_B \\ \dot{\omega}_B \\ \dot{v}_F \\ \dot{\omega}_F \\ \dot{v}_E \\ \dot{\omega}_E \end{Bmatrix} = \begin{Bmatrix} F_B \\ M_B - \tilde{\omega}_B I_B \omega_B \\ F_F - m_F\tilde{\omega}_F\tilde{\omega}_F r_F \\ M_F - \tilde{\omega}_F I_F \omega_F \\ F_E - m_E\tilde{\omega}_E\tilde{\omega}_E r_E \\ M_E - \tilde{\omega}_E I_E \omega_E \end{Bmatrix} \tag{9}$$

To couple the independent equations for the tanker, fixed boom, and boom extension to one another, constraint equations must be derived for the joints that connect each of the three components. The boom pivot is essentially a universal joint (perpendicular yaw and pitch rotations) and, as such, generates four algebraic constraint equations. The telescopic motion of the boom extension relative to the fixed boom can be modeled as a prismatic joint (one-dimensional translation) with five algebraic constraint equations. Using Lagrange multipliers, Eq. (9) can be combined with the nine constraint equations.

$$I_S\dot{p}_S - D^T\lambda = Q_S \tag{10}$$

$$\Phi(q_S) = 0 \tag{11}$$

where

$$\dot{\Phi}(q_S) \equiv Dp_S = 0 \tag{12}$$

At this point, the velocity transformation provides a means for expressing the generalized velocities of the system components in terms of the joint velocities.

$$p_S = B\dot{\eta} \tag{13}$$

Substitute Eq. (13) into Eq. (10) and multiply the resulting equation by the transpose of the velocity transformation matrix. The term containing the Lagrange multipliers is zero, based on the result of substituting Eq. (13) into Eq. (12). Then, the equations of motion for the coupled tanker/refueling boom system may be written in a form equivalent to that of Eq. (1).

$$B^T I_S B\ddot{\eta} = B^T(Q_S - I_S\dot{B}\,\dot{\eta}) \tag{14}$$

For integration with the existing model of the KC-135 tanker, the equation of motion shown in Eq. (14) is the preferred form.

C. Velocity and Acceleration Transformations

In the previous section, the coupling between the tanker and fixed boom and between the fixed boom and boom extension was implemented using the velocity transformation matrix and its derivative, the acceleration transformation matrix. In general, the components of these matrices are dependent on the types of joints used in the mechanism, as well as the geometry of the mechanism, and they represent the kinematical connections between the two joined bodies that relate the uncoupled coordinates of each body to the joint coordinates. For this particular model, the tanker is a floating body (no constraint equations), the joint between the tanker and the fixed boom is a universal joint, and the joint between the fixed boom and the boom extension is a prismatic joint. The tanker/boom system takes the form of an open-loop, single-chain geometry, with the sequence of joints described earlier. Therefore, the velocity transformation matrix takes the form shown in Eq. (15), in which

each of the components is a block matrix.

$$B = \begin{bmatrix} F_{BB} & 0 & 0 \\ F_{FB} & U_{FF} & 0 \\ F_{EB} & U_{EF} & P_{EE} \end{bmatrix} \tag{15}$$

The structure of the velocity transformation matrix in Eq. (15) reflects the topology (open chain, single branch) of the tanker/boom system. That is, the positions of the block matrices within the velocity transformation matrix are determined by the order in which the bodies are connected and by the type of joint that connects the bodies. By changing the block matrices in Eq. (15), one changes the kinematical connections between the bodies. The dimensions of each block matrix are determined by the type of joint that it represents. Because the number of joint velocities in a floating joint is the same as the number of coordinates for an uncoupled rigid body, all of the F block matrices have six rows and six columns. Universal joints have two joint velocities, one for each rotation, so the U block matrices have six rows and two columns. Only one joint velocity (translation) is needed for a prismatic joint and, therefore, the P block matrix has six rows and one column.

The structure of the block matrix for each type of joint can be predefined [6]; although for this investigation, the block matrices were derived directly from the kinematics of the bodies, because the definition of the kinematics for the boom pivot differed slightly from the standard definition of a universal joint. The general forms of the block matrices for the floating, universal, and prismatic joints, as defined in this model, are shown in Eqs. (16–18), respectively.

$$F_{XB} = \begin{bmatrix} A^{XI} & -A^{XB}\tilde{r}^{B}_{X/B} \\ 0 & A^{XB} \end{bmatrix} \tag{16}$$

$$U_{XF} = \begin{bmatrix} 0 & 0 \\ A^{XB}n^{B}_{\psi} & A^{XF}n^{F}_{\theta} \end{bmatrix} \tag{17}$$

$$P_{EE} = \begin{Bmatrix} n^{E}_{u} \\ 0 \end{Bmatrix} \tag{18}$$

IV. Coupled Model Aerodynamic and Equations of Motion Comparison

To compare the coupled model's aerodynamics to the previous existing models' aerodynamics, the tanker must be constrained to one-dimensional translation, as it is represented in the previous existing models. Aircraft translational motion is assumed to be only in the aircraft x-axis direction, and all aircraft rotational terms are set to zero. As a result, boom motion will not affect the tanker. Hardware saturation limits and the boom control system are neglected to compare unaltered equations of motion and aerodynamic characteristics. The ruddevator pitch angle normally includes two components: the commanded input from the boom operator and an autorotation deflection that is produced by the pantograph system. However, for this investigation, the operator input and autorotation are assumed to be implemented outside of the boom dynamic model. Both the BOPTT and AFIT models include functions that modify the ruddevator pitch angles as functions of boom yaw and pitch and operator input, but the functions included in the two models are not equivalent. Therefore, because it has not been determined which (if either) function is correct, pitch angles are directly input into this model. Also, hardware saturation limits (such as maximum and minimum boom pitch and yaw angles due to the aircraft and boom structure) and ruddevator saturation limits will be ignored. However, boom telescopic speed limits and extension position limits will be obeyed, because the extension rate is directly controlled by the boom operator. From [2], the nominal refueling position for the boom is at 30-deg pitch down, 0-deg yaw, and 12.2 ft of extension. These comparisons use typical automated aerial refueling simulation flight

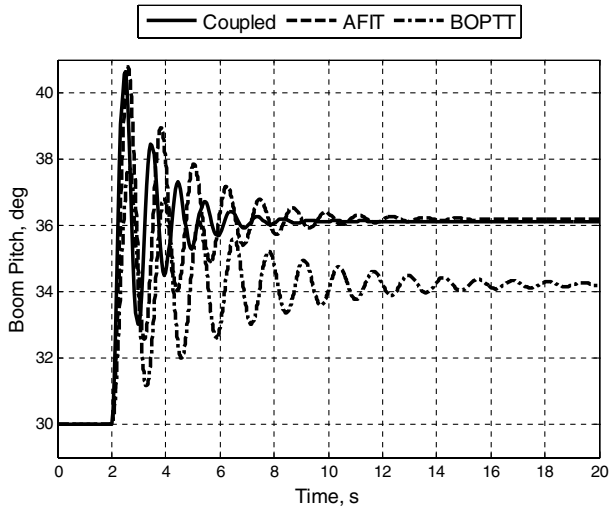

Fig. 5 Boom pitch response to a 6-deg symmetric ruddevator deflection about the trim.

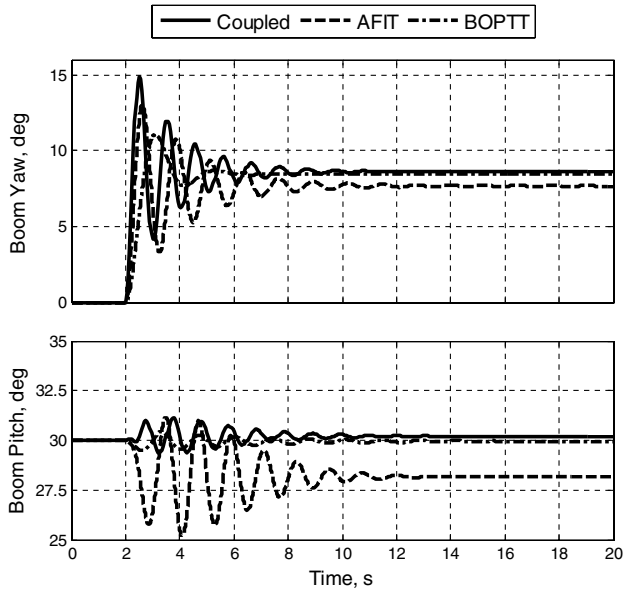

Fig. 6 Boom yaw and pitch responses to a 6-deg asymmetric ruddevator deflection about the trim.

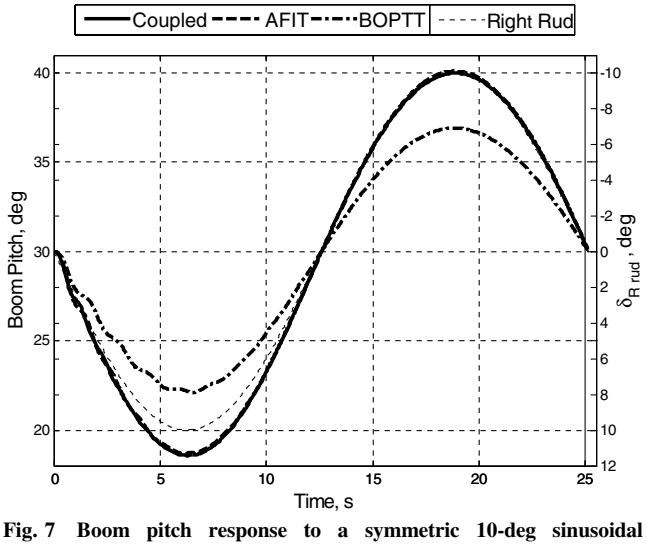

Fig. 7 Boom pitch response to a symmetric 10-deg sinusoidal ruddevator deflection about the trim.

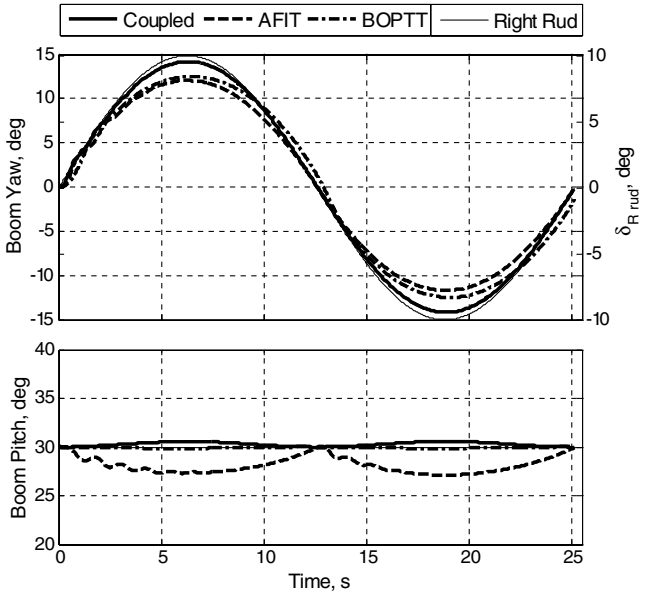

Fig. 8 Boom yaw and pitch response to an asymmetric 10-deg sinusoidal ruddevator deflection about the trim.

conditions at an aircraft speed of 670 ft/s and an altitude of 25,000 ft, using a standard atmosphere model. Test cases are simple step inputs of symmetric and asymmetric ruddevator deflections about trim conditions for pitch and yaw (Figs. 5 and 6) and sinusoidal inputs about trim conditions (Figs. 7 and 8).

V. Conclusions

One can see from the preceding analysis that no response is identical for any of the boom models, but they all exhibit the same trends. Differences exist between response damping and frequency and the resultant steady-state equilibrium angles because of the different approaches used to model the dynamics. The analytical model developed in this Note offers dynamic coupling and compatibility with an existing KC-135 tanker model that will improve aerial refueling modeling and simulation. Moreover, it exhibits sufficiently similar responses to the established BOPTT boom model. The coupled model, based on first principles rather than empirical aerodynamics or enigmatic experimental data, can be improved upon by eliminating current assumptions with more detailed information about the boom, such as its exact mass distribution and cross-sectional profile.

References

[1] Nalepka, J. P., and Hinchman, J. L., "Automated Aerial Refueling: Extending the Effectiveness of Unmanned Air Vehicles," AIAA Modeling and Simulation Technologies Conference and Exhibit, AIAA Paper 2005-6005, 2005.

[2] Campbell, T. G., Durkkley, G. D., Fletcher, J. J., Hutchings, S. J., Lee, J. H., Manley, T. J., Przybysz, J., and Roberts, R. W., "System Study of the KC-135 Aerial Refueling System, Vols. 1 and 2," M.S. Thesis, Department of Aeronautics and Astronautics, U.S. Air Force Institute of Technology, Wright-Patterson AFB, OH, 1989.

[3] Schulze, H. E., The Boeing Co., Seattle, WA, U.S. Patent for "Simplified Aircraft Boom Control Mechanism," Patent Number 2,960,295, Nov. 1960.

[4] Nikravesh, P. E., *Computer-Aided Analysis of Mechanical Systems*, Prentice–Hall, Upper Saddle River, NJ, 1988, p. 25.

[5] Jerkovsky, W., "The Structure of Multibody Dynamics Equations," *Journal of Guidance and Control*, Vol. 1, No. 3, 1978, pp. 173–182.

[6] Kim, S. S., and Vanderploeg, M. L., "A General and Efficient Method for Dynamic Analysis of Mechanical Systems Using Velocity Transformation," *Journal of Mechanisms, Transmissions, and Automation in Design*, Vol. 108, No. 2, 1986, pp. 176–182.